STATUS OF THE TRMM GROUND VALIDATION PROGRAM AT NASA GSFC

David B. Wolff[1,2]*, E. Amitai[1,3], D. A. Marks[1,3], D. Silberstein[1,3] and J. L. Pippitt[1,3]
[1]NASA GSFC, [2]Science Systems & Applications, Inc., [3]George Mason University

1. INTRODUCTION

The TRMM Ground Validation (GV) program at NASA GSFC has made considerable progress over the last several years. The GV program now has a complete record of Level I-III products from the Kwajalein and Melbourne, Florida sites. Current emphasis is to eliminate the remaining backlog for the Houston, Texas and Darwin, Australia sites. This paper provides details on the status of our data processing efforts, defines accuracy estimates of the various GV rain products, and shows comparisons between GV rain intensities and accumulations to satellite retrievals over the GV sites. We will show that the Version 6a TRMM TMI and PR retrievals are within ± 10% of the Version 5 GV estimates, at least over open ocean areas, away from contaminating effects of land and coastal regions. Table 1 provides details on the status of the Version 5 GV products.

Site	***Version 5 Completed***
Darwin, Australia (DARW)	12/1997-12/1998 12/2001
Houston, TX (HSTN)	12/1997 - 04/1999 08/1999 - 09/1999 01/2001 - 04/2002
Kwajalein, RMI (KWAJ)	1997-2004 (Current)
Melbourne, FL (MELB)	1997-2004 (Current)

Table 1: Status of Version 5 TRMM GV products.

2. VERSION 5 GV PRODUCT GENERATION

Table 2 provides a brief description of the standard GV products provided by NASA GSFC. The current version of these products (Version 5) is described more fully in Wolff et al. (2004). This version provides significant improvements in both rain intensity and accumulation estimates. The most significant improvements were made possible by: utilization of the Window Probability Matching Method (WPMM, Rosenfeld et al. 1994), for determining the radar reflectivity - rain rate relationships; improvements in the accumulation algorithm for integrating monthly rainfall; and some code fixes. Previous versions of the GV products used a bulk-adjustment scheme whereby the coefficient A of a first-guess power-law Z_e-R ($Z = AR^b$) relationship was adjusted to match the gauge and radar monthly accumulations. Such an approach provided unrealistic month-to-month variation in the statistics and variations in the adjusted Z_e-R relationships, especially in regions where available gauge data is limited and/or radar calibration was unstable.

* *Corresponding author address*: David B. Wolff, NASA GSFC, Code 912.1, Greenbelt, MD, 20771; e-mail: wolff@radar.gsfc.nasa.gov

Product	***Fields***	***Description***
1B-51	DZ, VR, ZDR	Original coordinates and fields; maximum range 230 km.
1C-51	CZ, DZ, VR	Original coordinates. CZ contains quality-controlled DZ field; maximum range 200 km; HDF format.
2A-52	Echo coverage	Percentage echo coverage with satellite coincidence; ASCII format.
2A-53	RR	Cartesian grid (2 km x 2 km, 151 x 151 pixels). Instantaneous rain intensity (mm hr^{-1}); maximum range 150 km; HDF format.
2A-54	Rain Type	Cartesian grid (2 km x 2 km, 151 x 151 pixels); rain type (stratiform or convective); maximum range 150 km; HDF format (Steiner et al. 1995)
2A-55	CZ	3-dimensional Cartesian grid (2 km x 2 km horizontal, 1.5 km vertical; 151 x 151 x 13 pixels); quality-controlled reflectivity; maximum range 150 km; maximum height 19.5 km; HDF format.
2A-56	RR	1-minute average gauge rain rates; one file per month, per gauge; ASCII format.
3A-53	R	Cartesian grid (2 km x 2 km).; 5-day integrated rainfall; maximum range 150 km; HDF format.
3A-54	R	Cartesian grid (2 km x 2 km).; monthly-integrated rainfall.; maximum range 150 km; HDF format.
3A-55	R	3-dimensional monthly structure with vertical profiles; HDF format.

Table 2: Description of the standard GV products: DZ is radar reflectivity; HDF is Hierarchical Data Format; VR is radial velocity; ZDR is differential reflectivity; CZ is quality controlled reflectivity; RR is rain rate; and R is rain accumulation.

The official GV rainfall products are developed in modular steps with distinct intermediate products. These steps include: (1) extracting quality-controlled radar data over the locations of rain gauges; (2) merging gauge and radar data in time and space; (3) performing an automated quality control (QC) of radar and gauge merged data; (4) deriving Z_e-R lookup tables for

converting observed radar reflectivities into rain intensities from the merged data; 5) application of the Z_e-R lookup tables to reflectivity data to produce rain rates, and 6) integration of the instantaneous rain maps into 5-day and monthly accumulation maps.

Reflectivity data from the 2A-55 product is extracted over the "calibration" rain gauge locations. Data from the 1.5 km and 3.0 km Constant Altitude Plan Position Indicator (CAPPI) levels are extracted from each radar volume scan (over the course of 1 month) from the 3 pixel x 3 pixel 'window' over each rain gauge location. Each radar pixel size is 2 km x 2 km and the extracted gauge data are obtained from the seven 1-minute rain rate averages, centered at the radar volume scan time, as explained in more detail by Amitai (2000).

The rain gauge data are then merged with the extracted reflectivities to create a second intermediate (merged) file for Z_e-R development. An automated QC algorithm (Amitai, 2000) is then applied to the combined radar and rain gauge data to determine which rain gauges (on a monthly scale) are reliable for the purposes of Z_e-R development. The reliability of a particular rain gauge is determined upon comparison with the associated radar data above the gauge location. When a gauge is considered unreliable for a particular month, all data from both the gauge and extracted radar pixels above that gauge are filtered from the merged file. This procedure ensures that only objectively determined "good" gauges are used in the monthly WPMM Z_e-R development. WPMM matches the probabilities of radar observed reflectivities Z_e and gauge measured rain intensity R in such a way that the probability density function (PDF) of the radar estimated R above the gauge will be identical to the PDF of the gauge rates on a monthly scale. Also, the resulting Z_e-R functions are found to be curved lines in log-log space rather than a straight-line power law (Rosenfeld et al., 1994).

For MELB, Monthly rainfall accumulation products are obtained by integrating the instantaneous rain rate maps over time. Integration parameters are defined by the time difference ΔT between successive radar volume scans. This approach assumes that instantaneous rain rates remain constant for the duration of the specific radar scan up to a maximum ΔT of 10 minutes. When ΔT exceeds 10 minutes, the rain rate map immediately following the data gap is integrated for 5 minutes. The 5-minute period was chosen as it represents the approximate time required to complete the WSR-88D volume scan. Gaps in excess of the specified ΔT are a source of error in the monthly rainfall products.

At KWAJ, lack of "good" gauge data provides unique circumstances that require different techniques than those employed at MELB. Here, *monthly* WPMM Z_e-R development is not performed due to the limited number of rain gauge sites. On average, data from less than seven good gauges are available each month. To circumvent this problem, and to create reliable Z_e and R distributions, QC radar and gauge data from the entire year of 2002 were combined. This procedure captures a full spectrum of precipitation events, and provides robust distributions for WPMM Z_e-R development. Because most of the good gauges are within 98 km of the Kwajalein S-band polarimetric radar, we also take a special approach to the Z_e-R development. To help mitigate range effects, gridded reflectivity data are extracted over the gauge locations from both the 1.5-km and 3.0-km CAPPI levels. Data from the 1.5-km (3.0-km) level are used in the Z_e distribution to develop a Z_e-R lookup table for the 15-98 km (98-150 km) range. By this technique, we are assuming that the Z_e-R distributions obtained from radar and gauges within 98-km can be used to develop Z_e-R lookup tables which are applied to the areas both inside and outside 98 km.

The monthly rainfall accumulation scheme employed at KWAJ is very similar to MELB in that the instantaneous rain rate maps are integrated over the time difference ΔT between successive radar volume scans; however, the maximum ΔT for integration is 15 minutes. Agin, if ΔT exceeds 15 minutes, the rain rates from the instantaneous map immediately following the gap are integrated for 10 minutes. The 10-minute period was chosen as it represents the approximate time between successive volume scans of the scanning strategy.

3. ACCURACY OF THE GV RAIN ESTIMATES

Due to vastly different scales between a radar "pixel" (about 1 km x 1 km at a range of 60 km for a 1° beam), and the 6" orifice of standard rain gauges, instantaneous comparisons between radar and gauges is not feasible; however, comparisons over a monthly scale are more robust and are presented here. Section 4 addresses the accuracy of GV rain intensity estimates, gridded over 0.5° x 0.5° boxes, compared to TRMM instantaneous retrievals.

Figure 1 provides comparisons of monthly radar estimated rainfall compared to gauges at MELB for August, 1988 during the Texas/Florida Under-flight Experiment (TEFLUN)-B. Figure 1a provides only *dependent* validation because the accumulations from gauges that are used to derive the WPMM Z_e-R relationship are plotted against the radar estimates. In order to provide truly *independent* validation, Fig. 1b provides comparisons of radar estimated monthly accumulations to gauges that were not used in the determination of the Z_e-R relationships (these gauges were placed by NASA specifically for validation purposes and are located at the NNN ranch 20 km west of the WSR-88D radar). Figure 1b shows this independent validation for this August, 1998, with radar to gauge biases (R/G) of 7% and highly-correlated accumulations. While this month provided particularly good agreement between the gauge measurements and radar estimates, which is not always the case; however, it can be stated that accuracies on the order of 10-15% are common at MELB.

Figure 2 provides comparisons between KWAJ radar estimates and gauge observations for the years of 2002 (panel a) and 2001 (panel b), respectively. Recall that 2002 is the period that was used to derive the WPMM relationships and thus provides only dependent validation; however, 2001 provides fully independent validation, and shows again excellent agreement between the gauge observations and radar estimates

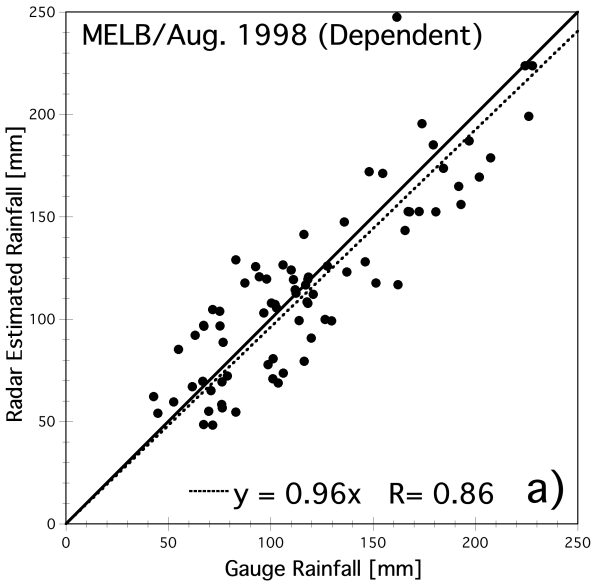

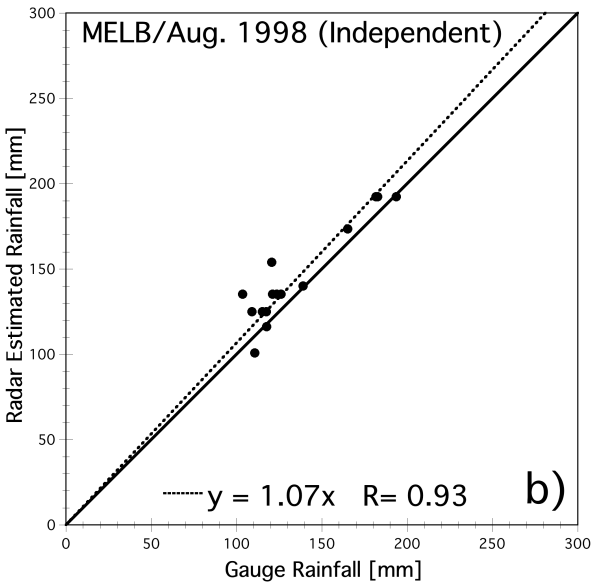

Fig. 1: a) Monthly rain gauge observations versus 2 km x 2 km radar estimates over the gauges for MELB, August 1998; and b) same as a), except gauges are not used in the derivation of the WPMM Z_e-R relationships and thus provide independent validation of the radar estimates.

(radar underestimate of about 4%). Other years (not shown) show similar agreement, but there are some notable differences, especially during periods when the radar calibration was biased relative to its 2002 state. There are several well known periods where the radar calibration is in question and hence work is underway to determine the absolute calibration can be better determined. It may be possible to use the polarimetric capability of the KWAJ radar to assist in this matter (Vivekanandan et al. 2003).

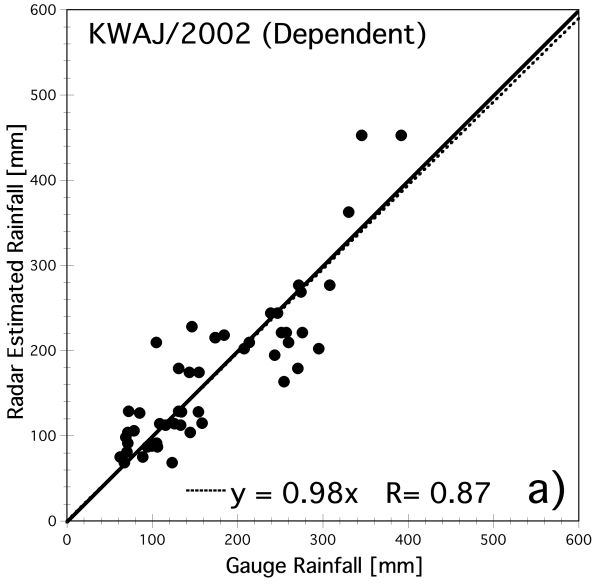

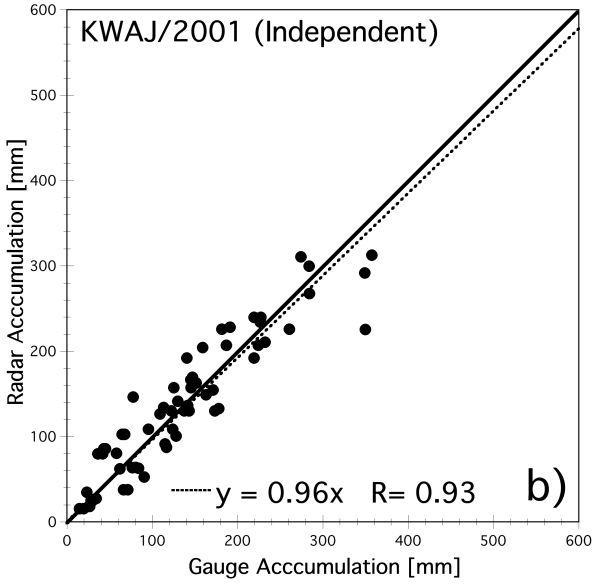

Fig. 3: a) Dependent validation of KWAJ monthly rain accumulations for 2002; and b) Independent validation of KWAJ monthly rain accumulations for 2001.

4. COMPARISON OF GV AND TRMM ESTIMATES

Finally, we provide a brief review of how well the GV estimates compare to TRMM satellite-retrieved estimates. We note that the TRMM data used in this analysis is from the Version 6a algorithms over the period January 2001 through April 2002, and do not

represent the "official" Version 6 estimates. The TRMM Science Data and Information System (TSDIS) is currently processing the official products and thus they are not available for comparison at the time of this writing.

From personal communication with the algorithm developers (Kummerow, Meneghini and Haddad), we do not believe that there will be significant changes in these comparisons for either the TMI or combined estimates over ocean; however, there may be some significant differences in the PR comparisons.

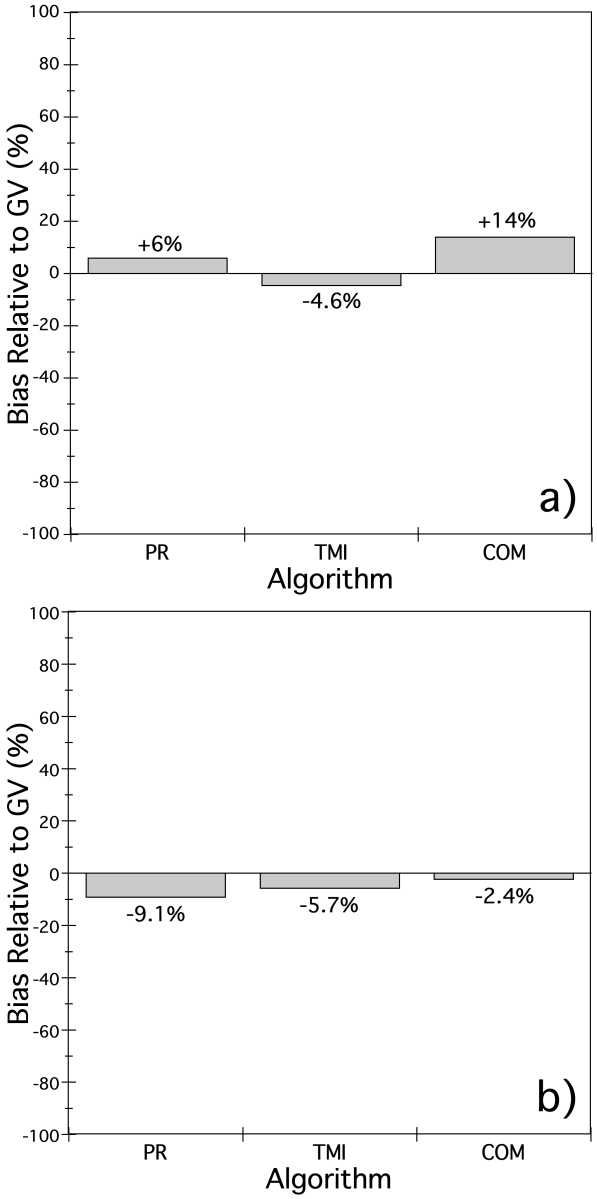

Fig. 3: Bias of TRMM satellite estimates relative to GV for the period Jan. 2001 through Apr. 2002 for a) KWAJ and b) MELB. These biases are calculated by comparing the mean rain rate over 0.5° x 0.5° pixels in the GV domain. Only pixels that were considered as "ocean" by the TRMM satellite algorithms are shown.

For brevity, we provide comparisons of our GV estimates over KWAJ and MELB only. Wolff et al. (2004) provide more details on these comparisons. For this analysis, estimates from the TRMM gridded 3G68 product were used to compare to GV rain intensities. The 3G68 global product provides the average rain rate in 0.5° x 0.5° pixels for the TRMM Microwave Imager (TMI), Precipitation Radar (PR) and Combined (COM) algorithms. The respective 3G68 pixels that lay over the respective GV sites were extracted and then compared to TRMM GV estimates obtained by de-resolving the 2 km x 2km 2A53 rain map pixels to the same grid as the 3G68 product. Thus, the comparison was pixel-matched in both time and space, removing sampling as a source of error in these comparisons.

Calculating a "bulk" bias, using all 0.5° pixels in which there was at least one PR footprint and fully contained a valid GV region, the TRMM estimates match well with GV estimates over open ocean. For KWAJ (see Fig. 3a), the PR, TMI and COM estimates were +6%, -4.6% and +14% of GV estimates, respectively. For MELB (see Fig. 3b), the PR, TMI and COM estimates were –9.,1%, -5.7% and –2.4% of GV estimates, respectively. Thus a strong convergence is evident not only the TRMM satellite estimates, but also between TRMM and GV.

Work is underway now to provide similar validation on a satellite "footprint" scale in order to better understand why the apparent regional differences in the estimates occur (Kummerow, personal communication).

5. REFERENCES

Amitai, E., 2000: Systematic variation of observed radar reflectivity-rainfall rate relations in the tropics. *J. Appl. Meteor*. (Special Issue on TRMM), **39**, 2198-2208.

Rosenfeld, D., D. B. Wolff, and E. Amitai, 1994: The window probability matching method for rainfall measurements with radar. *J. Appl. Meteor*., **33**, 682-693.

Steiner, M., R. A. Houze, and S. E. Yuter, 1995: Climatological characterization of three-dimensional storm structure from operational radar and rain gauge data. *J. Appl. Meteor.*, **34**, 1978-2007.

Vivekanandan, J., G. Zhang, S. M. Ellis, D. Rajopadhaya, and S. K. Avery, 2003: Radar reflectivity calibration using differential propagation phase measurement. *Radio Sci.*, **38**, 14/1-14/13.

Wolff, D. B, D. A. Marks, E. Amitai, D. S. Silberstein, B. L. Fisher, A. Tokay, J. Wang, and J. L. Pippitt, 2004: Ground Validation for Tropical Rainfall Measuring Mission (TRMM). *Jou. Atmos. Ocean. Tech.* Submitted.